STUDIA UBB CHEMIA, LXV, 3, 2020 (p. 89-100)
(RECOMMENDED CITATION)
DOI:10.24193/subbchem.2020.3.07

Na^+ - NH_4^+ CATION EXCHANGE STUDY ON TREATED ZEOLITIC VOLCANIC TUFF IN FIXED BED COLUMN

S. ANDRADA MĂICĂNEANU[a,*] and HOREA BEDELEAN[b]

ABSTRACT. In this work Na^+ - NH_4^+ cation exchange process was studied on various samples of treated zeolitic volcanic tuff (ZVT). Irrespective of the treatment applied (washing, NaCl, acid, thermal), the Na^+ concentration evolution closely mirrors the NH_4^+ concentration evolution indicating that Na^+ - NH_4^+ is the main ion exchange process that takes place. Cation exchange capacities (CEC) between 5.42 and 33.8 mg NH_4^+/g were obtained suggesting that not all treatments improved the ZVT's abilities to remove ammonium from wastewater. Changes in flow rate, Na^+ concentration, NH_4^+ concentration, ZVT amount, and ZVT grain size have all influenced the CEC in the considered system.

Keywords: *zeolitic volcanic tuff, clinoptilolite, ammonium, ion exchange, column, wastewater*

INTRODUCTION

Zeolitic volcanic tuff are materials containing different types of natural occurring zeolites in various amounts. Natural zeolites are low cost materials and are widespread around the world. American, Australian, Brazilian, Chilean, Chinese, Iranian, Serbian, Turkish, and Ukrainian natural zeolites are among the most studied ones.

Zeolites are porous hydrated aluminosilicates of alkali or alkaline earth metals. They have a three-dimensional crystalline lattice, consisting of SiO_4 and AlO_4 tetrahedra linked by shared oxygen atoms. The zeolite framework contains linked cages, cavities, and channels. The presence of Al^{3+} in the zeolite structure introduces a negative charge that is balanced by mono- and divalent cations, such as Na^+, K^+, Ca^{2+}, or Mg^{2+}. These cations loosely bound in the zeolite framework are called exchangeable cations. The

[a] *Madia Department of Chemistry, Indiana University of Pennsylvania, Indiana, PA 15705, USA*
[b] *Department of Geology, Babes-Bolyai University, 1 M. Kogălniceanu st., 400048, Cluj-Napoca, Romania*
**Corresponding author: Sanda.Maicaneanu@iup.edu*

exchangeable cations along with their coordinated water molecules are located on specific sites in the zeolite structure. Consequently, zeolites present specific properties: hydration reversibility, ion exchange ability, and adsorption-desorption capacity [1-6]. Clinoptilolite, member of the heulandite group (HEU) is one of the most abundant natural zeolite minerals tested widely in various applications [2,5].

Nitrogen is an essential nutrient, but when present in high concentration contribute to accelerated eutrophication of surface waters, dissolved oxygen depletion, and fish toxicity [4,7]. Ammonium is one of the forms of inorganic nitrogen that is a common water pollutant, usually present in industrial, municipal, and agricultural wastewater. Several processes are available to remove ammonium ions from wastewaters, such as biological processes, air stripping, breakpoint chlorination, chemical precipitation, adsorption, and ion exchange [1,3,4]. Zeolites' ion exchange ability, their high availability, low cost, and ease of application makes them ideal materials for ammonium removal from wastewater [4,7,8].

A survey of the last 10 years literature shows that ammonium removal from wastewater using zeolites remains a subject of great interest. Ammonium removal using Chinese zeolite [9,10], Iranian zeolite [11,12], high purity Serbian zeolite ion exchange combined with nitrogen release for microalgae cultivation [13], Australian zeolite [14], Cuban zeolite ion exchange coupled with bioregeneration by nitrification [15], Slovakian zeolite usage with recovery as liquid fertilizers [16], American and Japanese zeolites [17], and synthetic zeolite [18] were all studied over the last decade.

In the desire to increase natural zeolites' cation exchange capacity, several studies attempted the usage of treated zeolites for ammonium removal from wastewater. Therefore, Chinese clinoptilolite treated with NaCl and mixed with Na_2SiO_3 and powdered activated carbon was used successfully to remove ammonium from drinking water [19], Yemeni natural zeolite treated with NaCl solution of different concentrations at various temperatures showed improved removal efficiency [20], Chinese zeolite modified with MgO showed an increase of removal efficiency up to 97.6% [21], hydrated aluminum oxide modified Slovakian zeolite was used to simultaneously remove phosphate and ammonium [22], Chinese zeolite modified with potassium permanganate did not show an improvement in ammonium removal efficiency [23], NaOH modified zeolite showed a slight decrease on ammonium adsorption [24], highly concentrated NaCl, HCl, and NaOH treated clinoptilolite exhibited various outcomes depending on the initial concentration of ammonium solution [25], while a Chinese zeolite modified with 3.0 M $NaNO_3$ and calcined at 500°C, proved to be with 39.88% more efficient than the untreated sample [26].

The purpose of this work was to study the Na^+ - NH_4^+ cation exchange process in the zeolitic (clinoptilolitic) volcanic tuff (ZVT) – ammonium aqueous solution system and to examine the influence of various treatments applied to the zeolite sample over its cation exchange capacity (CEC) in a downflow mode operated column. The impact of flow rate, Na^+ concentration, NH_4^+ concentration, ZVT amount, and ZVT grain size over the CEC were also considered.

RESULTS AND DISCUSSION

Zeolitic volcanic tuff characterization

The zeolitic volcanic tuff (vitric tuff) sample used in this work was collected from a deposit located in the north-western part of the Transylvanian Depression (Măcicaș) that is included in the Dej Formation of Badenian age [27]. The bulk chemical analysis showed the acid character of the tuff with SiO_2 about 64%. The loss of ignition value indicates that more than 60% of the crystallized fractions of the tuff is formed by zeolites [3].

In Figure 1 a typical XRD diffractogram of the Măcicaș zeolitic tuff (**M-s**) is presented together with the diffractograms of samples treated with NaCl (**M-Na-22**, **M-Na-100**), HCl (**M-H2-22**), and thermally treated (**M-250**, **M-500**, **M-750**). The X-ray diffraction patterns show an almost similar mineralogical composition, with the clinoptilolite as the main mineralogical phase and small amount of quartz and albite. The appearance of the diffraction line of the **M-750** sample is slightly different from the others. Even if the mineral phases are approximately the same, the diffraction shows the presence of an amorphous phase, identified by a slightly vaulted shape of the diffraction line broad centered at 2θ = 20-25°. The peaks characteristic to the component minerals have a lower intensity, compared to other diffractions. All this suggests that at a temperature of 750°C, the structure of clinoptilolite begins to collapse after heating for 4 hours resulting in an amorphous phase [28]. The remaining peaks, after the clinoptilolite pattern had disappeared, belong to the minerals quartz and feldspar and possibly to the untransformed clinoptilolite (remnants).

FTIR spectra of the treated ZVT samples, for which the highest and lowest cation exchange capacity were calculated, are presented in Figure 2. The specific zeolite bands were identified as follows: 453 cm^{-1} (medium) O-T-O tetrahedral angular deformation; 608 cm^{-1} (medium) external vibrations of

T-O tetrahedral units coupled in rings; 669, 721, 790 cm^{-1} (weak) external T-O tetrahedral symmetric stretching; 1060 cm^{-1} (strong) external T-O tetrahedral asymmetric stretching; 1206 cm^{-1} (weak) internal T-O tetrahedral asymmetric stretching; 1636 cm^{-1} (weak) H-O-H angular deformation; 3448 cm^{-1} (medium) O-H stretching [3,29,30]. Additionally, the FTIR spectra of the treated samples displayed similar appearance, Figure 2, with specific features. Relative intensities of the specific bands decreased drastically, especially in case of **M-750** sample indicating structural changes in the ZVT structure. For the previous mentioned sample, the weak band at 1206 cm^{-1} almost disappeared, while for **M-H2-22**, the same band turned into a shoulder. OH/water bands in **M-750** became very weak and broad as expected for a sample treated at high temperature. 1060 cm^{-1} band position changes were recorded for **M-Na-100**, **M-H2-22**, **M-250**, and **M-750** to 1054, 1070, 1058, and 1073 cm^{-1} respectively.

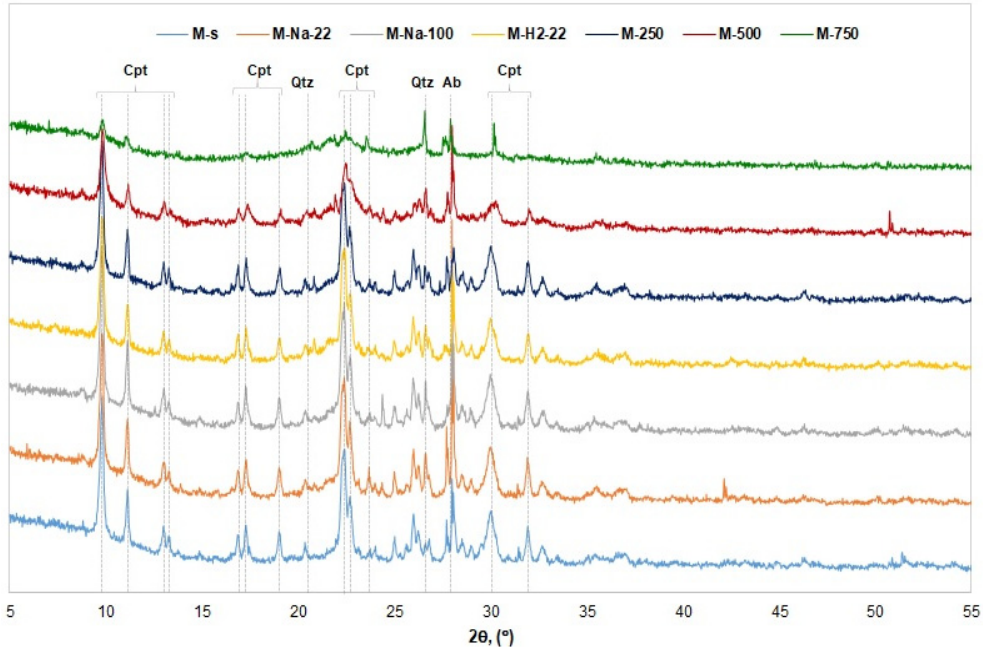

Figure 1. Powder X-ray diffractograms of some of the ZVT treated samples. Cpt - clinoptilolite, Qtz - quartz, Ab - albite.

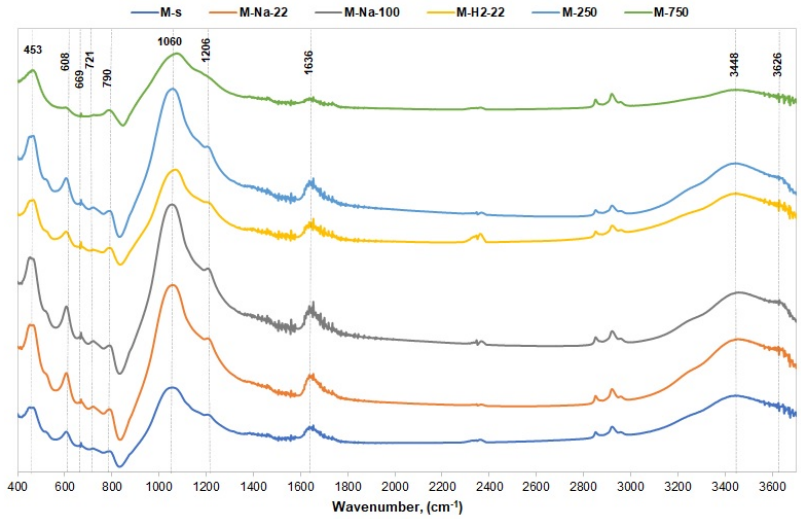

Figure 2. FTIR spectra of some of the ZVT treated samples.

Cation exchange results

As shown in Figure 3 (left), ZVT treatment plays an important role in the ammonium ion exchange process – *Experiment (1).* CEC increased when the zeolite was treated with NaCl, the maximum value of 33.8 mg NH_4^+/g being reached for the treatment realized at 100°C with 1 M NaCl solution. The acid treatment led to a decrease of CEC, the lowest value being determined for the treatment realized with 1 M H_2SO_4. As for the thermal treatment, CEC decreased abruptly with the increase of the temperature from 200 to 750°C. X-ray diffractograms and FTIR spectra showed that the ZVT structure underwent deterioration, especially during the 750°C treatment, therefore the CEC dropped to a minimum of 5.42 mg NH_4^+/g. In terms of concentrations evolution, Figure 3 (right), presented as a comparison between the treatments that gave the best and the worst results, it can be seen that the breakthrough point is at about 25 minutes for **M-750** and about 75 min for **M-Na-100**. The slope of the breakthrough curve is very steep in case of **M-750** indicating the early ZVT sample exhaustion. After the first step of the process (25 min and 100 mL effluent collected), the Na^+ concentration was determined to be 59.84 and 108.8 mg Na^+/L for **M-750** and **M-Na-100** respectively, showing that the availability of exchangeable sodium ions in the thermal treated deteriorated ZVT structure is very low. Na^+ concentration evolution mirrors closely the NH_4^+ concentration evolution as presented in Figure 3 (right).

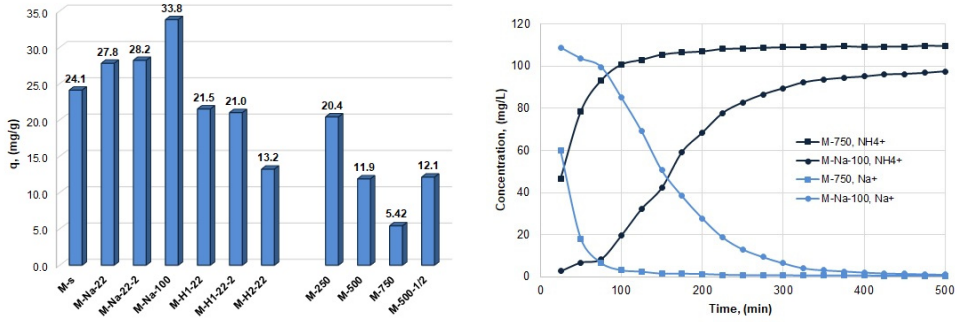

Figure 3. ZVT treatment influence over the ammonium CEC (left) and NH_4^+ and Na^+ concentrations evolution for **M-Na-100** and **M-750** (right); Experiment (1).

M-Na-100 ZVT sample was next used to test the influence of the flow rate over the ion exchange process – *Experiment (2)*. As the flow rate increased from 4 to 32 mL/min, the CEC decreased with about 30% from 33.8 to 23.3 mg NH_4^+/g respectively, Figure 4 (left). Breakthrough curves, presented as a comparison between the lowest and the highest flow rate, Figure 4 (right), exhibited a steeper slope and an early breakthrough point in case of 32 mL/min flow rate, which indicates a premature exhaustion of the ZVT sample when operated in these conditions. Following the sodium ions concentration, we observed that after the first step (100 mL effluent collected) about the same amount of ions was exchanged, while as the process further evolves the amount of Na^+ exchanged each step decreased for the 32 mL/min experiment indicating that diffusion limitations hinder the exchange process. Operating the column at a high flow rate leads to an underuse of the internal surface area of the ZVT ion exchanger.

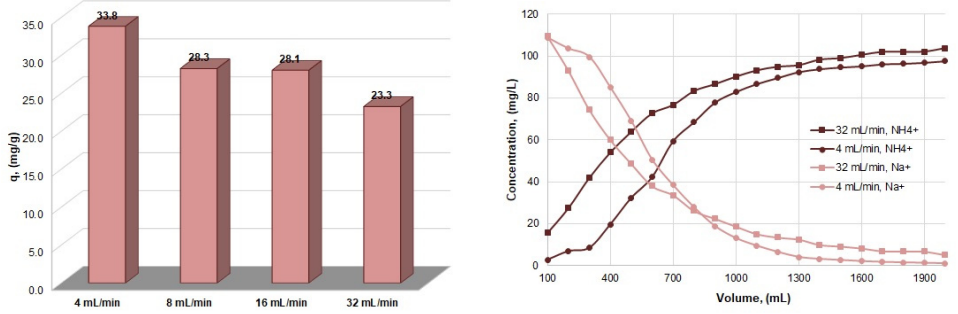

Figure 4. Ammonium CEC as a function of flow rate (left) and NH_4^+ and Na^+ concentrations evolution for **M-Na-100** (right); Experiment (2).

The influence of competitive sodium ions present in the ammonium solution – *Experiment (3)* – was also studied, using the **M-Na-100** sample. As depicted in Figure 5 (left), CEC slowly decreases from 28.3 to 22.6 mg NH_4^+/g as sodium ions concentration increases from 0 to 100 mg Na^+/L. As concentration increases further, up to 200 mg Na^+/L, no significant influence was observed. Breakthrough curves show similar profiles with a more gentler slope, Figure 5 (right), when 100 mg Na^+/L sodium ions were added indicating that the diffusion of Na^+ from the ZVT structure is limited by the increased amount of Na^+ in solution, therefore decreasing the rate of the ion exchange process.

Experiment (4) was conducted on the **M-Na-22** sample varying the amount of NH_4^+ present in solution. As presented in Figure 6 (left) the CEC increased with an increase in ammonium ions concentration, indicating the ability of ZVT sample to retain high amounts of ions. CEC increased from 17.4 to 31.1 mg NH_4^+/g as ammonium concentration in solution increased from 25 to 200 mg NH_4^+/L. The slope of the breakthrough curves became steeper when the NH_4^+ concentration increased, as presented in Figure 6 (right) for two concentrations. Sodium ions were not detected in solution after 425 min or 1700 mL eluent solution collected when the initial ammonium concentration was 200 mg NH_4^+/L suggesting the depletion of the exchangeable ions in the ZVT structure, which led to a cease of the ion exchange process.

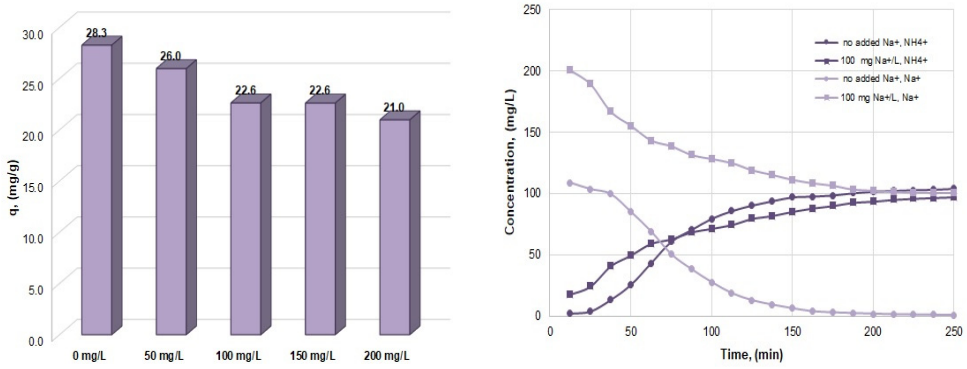

Figure 5. The influence of Na^+ presence over the ammonium CEC (left) and NH_4^+ and Na^+ concentrations evolution for **M-Na-100**; Experiment (3).

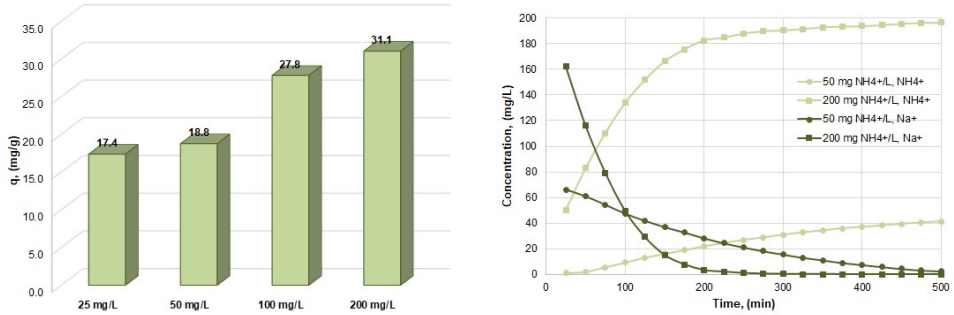

Figure 6. CEC as a function of the initial ammonium concentration (left) and NH_4^+ and Na^+ concentrations evolution for **M-Na-22** (right); Experiment (4).

For the final experiment, ZVT related parameters, amount and grain size were considered to study the Na^+ - NH_4^+ cation exchange process – *Experiment (5)*. As expected, the CEC decreased with an increase in the ZVT amount since for the same initial ammonium concentration a greater surface area is available, Figure 7 (left). With an increase in the grain size, CEC also decreased due to a decrease of the intraparticle diffusion rate, as most likely internal diffusion becomes rate limiting step, from 27.8 to 18.3 mg NH_4^+/g for 0.2-0.4 and 1.25-1.60 mm respectively. Breakthrough curves reflect this behavior, a gentler slope was recorded for the biggest particles used (1.25-1.60 mm). Sodium ions concentration evolution follows the same trend indicating that the amount of Na^+ exchanged decreased as the grain size increased.

CONCLUSIONS

The results obtained in the present study indicated that the only treatment applied to the ZVT that actually increased CEC is the NaCl treatment, the best results being obtained on the treatment realized at 100°C with a 1 M NaCl solution. As this treatment will generate supplementary costs with the heating agent and reflux equipment that have to be used, the closest alternative is carrying out the treatment process at room temperature, which also gives very good results in terms of CEC. Na^+ concentration evolution closely mirrors NH_4^+ concentration evolution for all experiments. The completion of the Na^+ - NH_4^+ cation exchange process was recorded only when the highest concentration of ammonium was tested (200 mg NH_4^+/L).

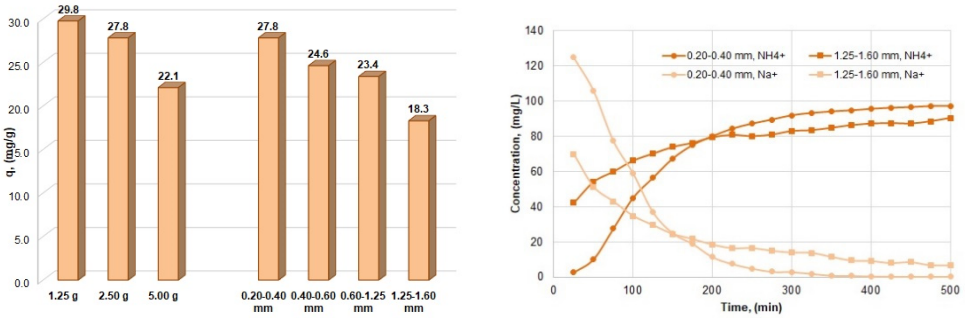

Figure 7. Influence of **M-Na-22** amount and grain size over the ammonium CEC (left) and NH_4^+ and Na^+ concentrations evolution for two grain sizes (right); Experiment (5).

EXPERIMENTAL

Zeolitic volcanic tuff

A sample of zeolitic volcanic tuff (ZVT) collected from Măcicaş (M) deposit (Cluj County, Transylvania, Romania) was used throughout this work. Raw ZVT was subjected to several treatments as follows:

(1) ***grinding*** followed by ***size separation*** to obtain the 0.20-0.40, 0.40-0.60, 0.60-1.00, 1.00-1.25, and 1.25-1.60 mm fractions;

(2) ***washing*** with distilled water and drying at 100±5°C for 24 h; samples of various grain size labeled **M-s** were obtained; these samples were further used to perform the subsequent treatments;

(3) ***NaCl treatment*** was realized using 1 M and 2 M NaCl solutions at room temperature, **M-Na-22** and **M-Na-22-2**, and under reflux at 100±5°C for 2 h, **M-Na-100**; a solid : liquid ratio of 1:10 and a stirring rate of 250 rpm were used; samples were washed with distilled water until no chlorine ions were identified in solution ($AgNO_3$ 0.01 M) and dried at 100±5°C for 24 h;

(4) ***acid treatment*** was realized using 1 M and 2 M HCl solutions, **M-H1-22** and **M-H1-22-2**, and 1 M H_2SO_4, **M-H2-22**, at room temperature for 2 h; a solid : liquid ratio of 1:10 and a stirring rate of 250 rpm were used; samples were washed with distilled water until no chlorine ions were identified in solution ($AgNO_3$ 0.01 M) and dried at 100±5°C for 24 h;

(5) ***thermal treatment*** was realized in a furnace at 250, 500, and 750°C for 4 hours, **M-250**, **M-500**, **M-750**, and 500°C for 2 h, **M-500-1/2**.

NaCl, HCl (36% w/w), H_2SO_4 (98% w/w), $AgNO_3$ used were of analytical purity (Merck, Germany).

ZVT characterization

XRD analyses of ZVT samples were performed using a D8 ADVANCE Bruker diffractometer, CuKα anticathode. The diffractograms were recorded from 5° to 60°, 2θ degree. The analytic conditions were 40 kV, 40 mA, and a step of 0.02 degrees/min.

FTIR analyses were performed on dried samples prepared by encapsulating 1.2 mg of finely grounded particles in 300 mg of KBr. Infrared spectra were obtained using a JASCO 615 FTIR spectrometer 400-4000 cm^{-1} (resolution, 2 cm^{-1}).

Ion exchange experiments

Ammonium removal experiments were conducted in a 20 mm diameter (450 mm length) column equipped with a glass frit in down flow mode. Glass wool fibers (layer of about 1.0 mm thickness) were set on the frit before the ZVT was added to avoid pores blockage. The liquid level in the column and the flow rate were maintained constant using a peristaltic pump and the column's stopcock.

NH_4Cl and NaCl of analytical purity (Merck, Germany), and distilled water were used to prepare stock solutions of 1000 mg/L. Solutions in 25-200 mg NH_4^+/L range and 50-200 mg Na^+/L were further prepared.

Ion exchange experiments were conducted as follows:

Experiment (1) – ZVT treatment – all prepared samples, 0.20-0.40 mm and 2.5 g, were tested using a 100 mg NH_4^+/L solution and a flow rate of 4 mL/min (no sodium added);

Experiment (2) – flow rate – **M-Na-100** sample, 0.20-0.40 mm and 2.5 g, was tested using a 100 mg NH_4^+/L solution and a flow rate in the 4-32 mL/min range (no sodium added);

Experiment (3) – sodium ions presence in solution – **M-Na-100** sample, 0.20-0.40 mm and 2.5 g, was tested using a 100 mg NH_4^+/L solution, a flow rate of 8 mL/min, and sodium ions concentration in the 50-200 mg/L range;

Experiment (4) – ammonium ion concentration – **M-Na-22** sample, 0.20-0.40 mm and 2.5 g, was tested using a flow rate of 4 mL/min and ammonium ion concentrations ranging from 25 to 250 mg/L (no sodium added);

Experiment (5) – zeolite amount and grain size – **M-Na-22** sample of all grain sizes, as listed in the previous section, were tested using a flow rate of 4 mL/min and a 100 mg NH_4^+/L solution, while the 0.20-0.40 mm **M-Na-22** sample was also tested using 1.25, 2.50, and 5.00 g in the same conditions.

The general cation exchange reaction taking place in the considered system is:

$$\text{M-}\left(K^+, Na^+, Ca^{2+}, Mg^{2+}\right) + NH_4^+ \rightleftharpoons \text{M-}(NH_4^+) + (K^+, Na^+, Ca^{2+}, Mg^{2+})$$

while for the samples treated with NaCl, is expected that the prevailing reaction is:

$$\text{M-}(Na^+) + NH_4^+ \rightleftharpoons \text{M-}(NH_4^+) + Na^+$$

Ammonium and sodium ions concentrations were determined using an ion chromatograph, Metrohm 761 Compact IC (Switzerland), equipped with a Metrosep C2-250 cation column ($t_{R,sodium}$ = 7.6 min; $t_{R,ammonium}$ = 8.7 min). Eluent composition for the above-mentioned column is 4.0 mmol/L tartaric acid and 0.75 mmol/L dipicolinic acid prepared in ultrapure degassed water and filtrated through 0.45 μm cellulose filtrating disks using a vacuum filtering system. Ammonium and sodium ions concentration in solution was determined at the outflow of the column every 100 mL, up to 2000 mL for all experiments. Prior to the injection in the chromatograph, samples were filtrated using 0.45 μm cellulose syringe filters.

Tartaric acid, dipicolinic acid of analytical purity (Merck, Germany), sodium standard solution ($NaNO_3$ in HNO_3, 1000 mg/L), ammonium standard solution (NH_4Cl in H_2O, 1000 mg/L) CentiPUR® Milipore Sigma, and ultrapure water were used.

An additional initial test in which beside Na^+ and NH_4^+, concentrations of Li^+, K^+, Ca^{2+}, and Mg^{2+} were determined using the method described above (initial concentration of 100 mg NH_4^+/L, **M-Na-22**) was performed. Lithium, potassium, and magnesium ions were not identified in any of the effluent samples collected, while calcium ions were determined to be about 7.8% of the initial ammonium concentration. Therefore, for the main experiments only Na^+ and NH_4^+ concentrations monitoring was considered.

The effectiveness of the ion exchange process was evaluated using the evolution of NH_4^+ and Na^+ concentrations in time and the operating exchange capacity, CEC, *q* (mg NH_4^+/g), calculated using the following equation:

$$q_t = \left[\frac{(C_i - C_t)}{m} \cdot \frac{V}{1000}\right] + q_{t-1}$$

where, q_t and q_{t-1} are the ammonium operating cation exchange capacities at times *t* and *t-1*, respectively, in (mg/g); C_i and C_t are the ammonium concentrations, initial and time *t*, respectively, in (mg/L); *m* is the amount of ZVT sample in (g); *V* is the sample volume, in (L).

REFERENCES

1. A. Hedstrom; *J. Environ. Eng.,* **2001**, *127*, 673-681.
2. F. Cakicioglu-Ozkan; S. Ulku; *Microporous Mesoporous Mater.*, **2005**, *77*, 47-53.
3. A. Maicaneanu; H. Bedelean; S. Burca; M. Stanca; *Sep. Sci. Technol.*, **2011**, *46*, 1621-1630.

4. M. Turan; *Nanosci. Nanotechnol*., **2015***,* 477–504.
5. K. Stocker; M. Ellersdorfer; M. Lehner; J.G. Raith; *BHM*, **2017**, *162*, 142-147.
6. P.J. Reeve; H.J. Fallowfield; *J. Environ. Manage*., **2018**, *205*, 253-261.
7. J. Huang; N.R. Kankanamge; C. Chow; D.T. Welsh; T. Li; P.R. Teasdale; *J. Environ. Sci.*, **2018**, *63*, 174-197.
8. Z. Ghasemi; I. Sourinejad; H. Kazemian; S. Rohan; *Rev. Aquacult*., **2018**, *10*, 75-95.
9. H. Huang; X. Xiao; B. Yan; L. Yang; *J. Hazard. Mater*., **2010**, *175*, 247–252.
10. H. Huang; L. Yang; Q. Xue; J. Liu, L. Hou; L. Ding; *J. Environ. Manage*., **2015**, *160*, 333-341.
11. R. Malekian; J. Abedi-Koupai; S.S. Eslamian; S.F. Mousavi; K.C. Abbaspour; M. Afyuni; *Appl. Clay Sci*., **2011**, *51*, 323–329.
12. F. Mazloomi; M. Jalali; *J. Environ. Chem. Eng*., **2016**, *4*, 240-249.
13. G. Markou; D. Vandamme; K. Muylaert; *Bioresour. Technol.*, 2014, 155, 373-378.
14. G.J. Millar; A. Winnett; T. Thompson; S.J. Couperthwaite; *J. Water Process Eng*., **2016**, *9*, 47-57.
15. T.H. Martins; T.S.O. Souza; E. Foresti; *J. Environ. Chem. Eng*., **2017**, *5*, 63-68.
16. I. Sancho; E. Licon; C. Valderrama; N. de Arespacochaga; S. López-Palau; J.L. Cortina; *Sci. Total Environ*., **2017**, *584-585*, 244-251.
17. H-F. Chen; Y-J. Lin; B-H. Chen; I. Yoshiyuki; S. Y-H. Liou; R-T. Huang; *Minerals*, **2018**, *8*, 499.
18. W. He; H. Gong; K. Fang; F. Peng; K. Wang; *J. Environ. Sci.*, **2019**, *85*, 177-188.
19. M. Li; X. Zhu; F. Zhu; G. Ren; G. Cao; L. Song; Desalination, **2011**, *271*, 295-300.
20. A. Alshameri; A. Ibrahim; A.M. Assabri; X. Lei; H. Wang; C. Yan; *Powder Technol*., **2014**, *258*, 20-31.
21. J. Guo; Desalin. *Water Treat*., **2016**, *57*, 5452-5463.
22. D. Guaya; C. Valderrama; A. Farran; C. Armijos; J.L. Cortina; *Chem. Eng. J*., **2015**, *271*, 204-213.
23. H. Guo; X.Y. Zhang; J.L. Liu; *Chem. Eng. Trans*., **2016**, *55*, 163-168.
24. Y. He; H. Lin; Y. Dong; Q. Liu; L. Wang; *Chemosphere*, **2016**, *164*, 387395.
25. K. Stocker; M. Ellersdorfer; M. Lehner; A. Lechleitner; J. Lubensky; J.G. Raith; *Microporous Mesoporous Mater*., **2019**, *288*, 109553.
26. H. Fua; Y. Lia; Z. Yua; J. Shena; J. Lia; M. Zhanga; T. Dinga; L. Xua; S.S. Leeb; *J. Hazard. Mater*., **2020**, *393*, 122481.
27. F. Mumpton; *Am. Mineral.,* **1960**, *45*, 351–369.
28. R. Plesa Chicinas; H. Bedelean; A. Maicaneanu; *Stud. Univ. Babes-Bolyai. Chem.*, **2016**, *61*, 243-254.
29. G. Rodriguez-Fuentes; A. R. Ruiz-Salvador; M. Picazo; G. Quintana; M. Delgado; *Microporous Mesoporous Mater*., **1998**, *20*, 269-281.
30. M. Mozgawa; *J. Mol. Struct*., **2000**, *555*, 299-304.